EPJ Web of Conferences **175**, 05002 (2018) https://doi.org/10.1051/epjconf/201817505002
Lattice 2017

Chiral Extrapolations of the $\rho(770)$ Meson in $N_f = 2 + 1$ Lattice QCD Simulations

R. Molina[1,⋆], *B.* Hu[2], *M.* Doering[2,3,⋆⋆], *M.* Mai[2], and *A.* Alexandru[2,⋆⋆⋆]

[1] *Instituto de Física, Universidade de São Paulo, São Paulo, 05508-090, Brazil*
[2] *The George Washington University, Washington, DC 20052, USA*
[3] *Thomas Jefferson National Accelerator Facility, Newport News, VA 23606, USA*

Abstract. Several lattice QCD simulations of meson-meson scattering in p-wave and Isospin = 1 in $N_f = 2 + 1$ flavours have been carried out recently. Unitarized Chiral Perturbation Theory is used to perform extrapolations to the physical point. In contrast to previous findings on the analyses of $N_f = 2$ lattice data, where most of the data seems to be in agreement, some discrepancies are detected in the $N_f = 2 + 1$ lattice data analyses, which could be due to different masses of the strange quark, meson decay constants, initial constraints in the simulation, or other lattice artifacts. In addition, the low-energy constants are compared to the ones from a recent analysis of $N_f = 2$ lattice data.

1 Introduction

Unitarized Chiral Perturbation Theory (UChPT) is a nonperturbative method which combines the constraints from coupled-channel unitarity and chiral symmetry. In this approach, several resonances such as the ρ and σ mesons are identified with poles of the scattering amplitude in the complex-energy plane. Instead of expanding the scattering amplitude in powers of momenta, as it is usually done in Chiral Perturbation Theory, an expansion of its inverse is preferred. This so-called inverse amplitude method was introduced in Ref. [1] and extended in Refs. [2–8]. In this approach, the $O(p^2)$ and $O(p^4)$ chiral Lagrangians [9, 10] provide the kernel of the scattering equation. While the lowest order term qualitatively leads to the generation of the scalar resonances, the $O(p^4)$ chiral Lagrangian, which depends on the low energy constants, is responsible for the generatation the vector-meson resonances [11]. As a result, the UChPT model with $O(p^2)$ and $O(p^4)$ chiral Lagrangians dynamically generates the scalar- and vector-meson resonances and describes scattering data up to 1.2 GeV [11].

The UChPT model can be implemented in the finite volume by imposing that the scattering states can only have discrete momenta. This formalism, developed in Refs. [12–15] is equivalent to the Lüscher approach up to contributions kept in Ref. [13] that are exponentially suppressed with the

⋆The authors thank the Hadron Spectrum Collaboration, J. Bulava and L. Leskovec for providing the results of the lattice simulations including covariance matrices. e-mail: ramope@if.usp.br
⋆⋆M. D. gratefully acknowledges support from the NSF/Career award no. 1452055 and from the U.S. Department of Energy, Office of Nuclear Physics under Contract No. DE-AC05-06OR23177 and grant no. DE-SC0016582.
⋆⋆⋆A.A. is supported in part by the National Science Foundation CAREER grant PHY-1151648 and by U.S. Department of Energy grant DE-FG02-95ER40907. A.A. gratefully acknowledges the hospitality of the Physics Departments at the Universities of Maryland and Kentucky, and the Albert Einstein Center at the University of Bern.

cube volume. In Ref. [16] the method is generalized to the cases of moving frames and partial-wave-mixing in coupled channels.

The above model was used to analyze the energy levels extracted from a lattice simulation of the GWU group of $\pi\pi$ scattering in p-wave in two flavours, see Ref. [17]. The result turned out to be in agreement with other $N_f = 2$ lattice simulations. Later, this study was extended to other lattice data sets in $N_f = 2$ [18]. Two common features were observed from the analyses: 1) The error ellipses of the low energy constants have a common overlap; 2) All extrapolations led to a consistently lower ρ mass (~ 60 MeV) than its physical value. Furthermore, the $N_f = 2$ simulation from the RQCD group at a pion mass close to the physical mass, 149 MeV, gives a ρ meson mass of around 710 MeV [19].

While it is possible that the reason for discrepancy lies in the scale settings or other lattice QCD artifacts, in Refs. [17, 18], it was shown that the discrepancy can also be accomodated in terms of the strange quark. There, by adding the $K\bar{K}$ channel a posteriori in the analysis of the $N_f = 2$ lattice data, it was observed that the ρ mass shifts upward in around 60 MeV, consistently for the different lattice data sets, being thus a likely reason for discrepancy.

In this work, we analyze the lattice data from simulations of the ρ meson phase shifts in $N_f = 2+1$ flavours, which have been carried out in recent years [20–29]. The theoretical framework is the one- and two- coupled channel UChPT model of Refs. [17, 18]. Chiral extrapolations to the physical point are provided for the various simulations. The values of the low energy constants (LECs) are discussed. Finally, the role of the strange quark in the $N_f = 2 + 1$ lattice simulations is investigated.

2 Formalism

The two-channel scattering equation reads, in the UChPT model, as follows [11],

$$T = V_2[V_2 - V_4 - V_2 G V_2]^{-1} V_2 \,, \tag{1}$$

where V_2 and V_4 are 2×2 matrices which contain the transition potentials derived from the $O(p^2)$ and $O(p^4)$ Lagrangians of the ChPT expansion [9, 10]. With the channel ordering $(\pi\pi, K\bar{K})$ these potentials, projected on $I = 1$ and $L = 1$, V_2 and V_4, are [17]

$$-\begin{pmatrix} \frac{2p_1^2}{3f_\pi^2} & \frac{\sqrt{2}p_2 p_1}{3f_K f_\pi} \\ \frac{\sqrt{2}p_2 p_1}{3f_K f_\pi} & \frac{p_2^2}{3f_K^2} \end{pmatrix} \quad \text{and} \quad -\begin{pmatrix} \frac{8p_1^2(2\hat{l}_1 M_\pi^2 - \hat{l}_2 W^2)}{3f_\pi^4} & \frac{8p_1 p_2 (L_5(M_K^2+M_\pi^2) - L_3 W^2)}{3\sqrt{2}f_\pi^2 f_K^2} \\ \frac{8p_1 p_2 (L_5(M_K^2+M_\pi^2) - L_3 W^2)}{3\sqrt{2}f_\pi^2 f_K^2} & \frac{4p_2^2(10\hat{l}_1 M_K^2 + 3(L_3 - 2\hat{l}_2)W^2)}{9f_K^4} \end{pmatrix}, \tag{2}$$

respectively. In the above equation, $p_i = \frac{\sqrt{(W^2-(m_1+m_2)^2)(W^2-(m_1-m_2)^2)}}{2W}$ for the channel i, W is the center-of-mass energy, and $m_{1,2}$ refers to the masses of the mesons $1, 2$ in the i channel. In the transition potential of Eq. (2), four distinct combinations of LECs are involved, $\hat{l}_1$, $\hat{l}_2$, L_3 and L_5, where $\hat{l}_1 = 2L_4 + L_5$, and $\hat{l}_2 = 2L_1 - L_2 + L_3$. Note that in the present notation the $\hat{l}_i$ are not the canonical SU(2) LECs but combinations of SU(3) LECs. In Eq. (1), G is a diagonal matrix whose elements are the two-meson loop functions, which are evaluated using dimensional regularization. The dependence on the subtraction constant in the case of the ρ meson can well be absorbed in the values of the LECs [18]. The meson decay constant dependence on the pion mass is taken from Ref. [6], where f_π, f_K are fitted in an analysis of combined lattice and experimental data.

The elements T_{ij} of the scattering amplitude are related to S-matrix elements as follows,

$$T_{ij} = -\frac{8\pi W}{2i\sqrt{p_i p_j}}(S_{ij} - \delta_{ij}) \,, \quad \text{where} \quad S = \begin{pmatrix} \eta e^{2i\delta_1} & i(1-\eta^2)^{1/2} e^{i(\delta_1+\delta_2)} \\ i(1-\eta^2)^{1/2} e^{i(\delta_1+\delta_2)} & \eta e^{2i\delta_2} \end{pmatrix}. \tag{3}$$

When the UChPT model is fitted to the experimental data for $\pi\pi$ and πK phase shifts, similarly as in Ref. [30], we obtain the values for the LECs in Eq. (2) given in the last row of Table 1. In what follows, we will refer to this fit as "Experimental".

The UChPT model can be adapted to the conditions of the lattice simulations, see Refs. [12–17]. While in Ref. [17] the eigenenergies were fitted, here we directly fit the extracted phase shifts. The correlation between energy W and phase shift $\delta(W)$ is taken into account, and also the correlations between eigenenergies themselves if available. We refer the reader to Ref. [31] for a more complete description of the fitting procedure.

3 Results

The lattice data for p-wave $\pi\pi$ phase shifts in $I = 1$ of Refs. [20–22, 24, 27, 28] are fitted by the UChPT model described in the previous section. We skip the analysis of the data from Ref. [29] because they have large uncertainties. Note that in the two-coupled-channel problem, see Eq. (2), there are now four parameters for the minimization problem. When performing the fits strong non-trivial correlations between the parameters appear and many different χ^2 minima are found. Then, it becomes necessary to restrict the model to study the parametrization and chiral behaviour. With that in mind, four different strategies (a), (b), (c), and (d) are pursued, which are described below.

Fit (a) – fixed L_3, L_5. This strategy, with two LECs L_3 and L_5 fixed to their values obtained by fitting phase shifts from experiment [17, 18], is identical to the approach of Refs. [17, 18]. The result for the extrapolated phase shifts at the physical point, in comparison to the lattice and experimental data, is shown in Fig. 1. Continuous lines represent the result from the two-channel SU(3) fits. Here one-channel SU(2) fits were also done, and the result is depicted with dashed lines. Both, one- and two-coupled-channel fits give very similar extrapolated phase shifts, which demonstrates that the explicit dynamics of the $K\bar{K}$ channel can be almost fully absorbed in the LECs of the SU(2) fit. A more detailed discussion on the SU(2) UChPT fits can be found in the Appendix of Ref. [31].

As shown in Table 1, see the $\chi^2_{\text{d.o.f}}$, the lattice data are well described by the SU(3) UChPT model. The extrapolated phase shifts, as Fig. 1 shows, agree with the experiment for the Wilson15 and Bulava16 data. However, in the case of the Dudek13 [20] data, the extrapolated phase shift is at slightly lower energies than the experiment, for Aoki11 the extrapolation is at higher energies, and for the Alexandrou17 data, is much lighter than the one from experiment. In Fig. 2 (left), results for (m_ρ, g) for different lattice data sets are presented. Empty and filled symbols stand for SU(2) and SU(3) analyses, respectively. The experimental point is indicated as "phys.". For the Bulava16, Wilson15 and Dudek13 data, the values of m_ρ and g in the SU(3) fits are close to the physical value, with larger discrepancies for the Alexandrou17 and Aoki11 data sets.

Error ellipses for the $(\hat{l}_1, \hat{l}_2)$ parameters, in the SU(3) analyses are shown in Fig. 3 (left). We note that the error ellipses do not have an as clearly common overlap region as in the analysis of $N_f = 2$ data of Ref. [18]. In particular, the ellipses of Aoki11 and Alexandrou17 are separated from the bulk of other $N_f = 2 + 1$ lattice data and the $N_f = 2$ result from Lang11. In the analysis of the $N_f = 2 + 1$ lattice data of Ref. [27] (Fu16), where we found some discrepancies with other sets of lattice data for similar pion masses, and also unusually large differences with the experimental data when the extrapolations are done, is discussed in Appendix of Ref. [31].

Fit (b) – free L_3, L_5. Before going into detail we want to make here a remark. The LECs that appear in the UChPT model are not only constraint by data in the p-wave, Isospin = 1, strangeness = 0 channel, but also in other channels, Isospin = 0, strangeness = −1, etc. This implies that by fitting with only data in the ρ channel can lead (and leads) to multiple solutions. Because of this, one can always choose one solution which has an extrapolation to the physical point compatible with the experiment (this would be almost equivalent to fitting the lattice data in combination with the

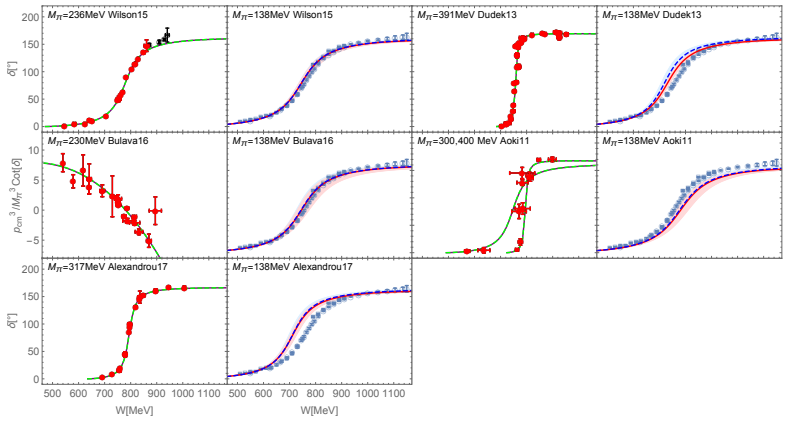

Figure 1. Phase shifts obtained for the minimization strategy (a) described in the text. Lattice data included in the fit [20–22, 24, 28] are shown in red, together with their extrapolations to the physical point (red and dashed-blue curves), and in comparison to the experimental data (blue) [32]. In all plots, solid (dashed) lines show the results using the two-channel SU(3) model (one-channel SU(2) model).

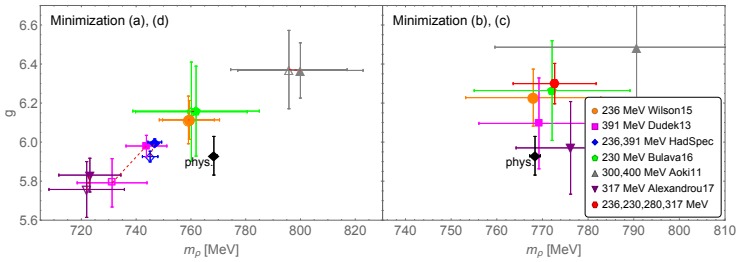

Figure 2. The $\rho\pi\pi$ coupling constant, g vs. m_ρ, for the extrapolation to the physical point obtained from the analysis of the different lattice data sets. Left: minimization strategies (d) -blue diamond-, and, (a) -all other symbols; Right: strategies (c) -red hexagon and (b) -all other symbols. In the left figure, empty and filled symbols represent SU(2) and SU(3) analyses respectively. The experimental point is indicated as "phys.".

experimental data). However by no means this is a good prediction of the extrapolation of the lattice data. In order to have a good prediction of the lattice data at the physical point, more data are needed, as data for several pion masses, or in several channels, pion decay constants used etc. Otherwise it is convenient to impose extra constraints in the LECs, as for example it is done in strategy (a). This strategy will be useful to show that when allowing that the different lattice data sets have extrapolated phase shifts compatible with experiment, quite different values of the LECs are obtained for some of those, which is not possible. We choose a minimum in which the predicted χ^2 evaluated with the *experimental* phase shifts is small, i.e., a minimum with excellent chiral extrapolation, and compare the resulting values of L_3 and L_5 with strategy (a) for consistency.

All extrapolated phase shifts for the different lattice data sets agree very well with experiment (not shown here, see Ref. [31] for further details) and the $\chi^2_{\rm d.o.f}$ obtained is close to one for most of the lattice data sets, see Table 1. However, there are clear discrepancies in the LECs for some of the lattice data sets. In Fig. 3 (right), the error ellipses for the L_3, L_5 parameters obtained from minimization

Table 1. Low-energy constants and $\chi^2_{\text{d.o.f.}}$ obtained in minimization strategies (a), (b), (c) and (d) for the lattice data from Refs. [20–22, 24, 28]. The superscript (f) indicates parameters held fixed at their experimental values. In the last two rows, the results from Ref. [17] and from the fit to the experimental data [30] are shown.

		Strategy (a)			Strategy (b)				
		$(L_3 = -3.01^{(f)},\ L_5 = 0.64^{(f)})$							
	M_π(MeV)	$\hat{l}_1$	$\hat{l}_2$	$\chi^2_{\text{d.o.f.}}$	$\hat{l}_1$	$\hat{l}_2$	L_3	L_5	$\chi^2_{\text{d.o.f.}}$
Wilson15	236	3.7(1.2)	−3.2(3)	0.9	$4.7^{+1.2}_{-0.8}$	$-3.0^{+0.2}_{-0.9}$	$-3.4^{+1.7}_{-0.2}$	$-0.4^{+0.6}_{-1.0}$	1.0
Dudek13	391	1.8(5)	−3.7(3)	1.2	$5.4^{+0.9}_{-0.1}$	$-7.4^{+0.6}_{-0.1}$	$+4.3^{+0.3}_{-0.04}$	$-3.8^{+0.7}_{-0.1}$	1.3
Bulava16	230	5(2)	−3.1(4)	1.1	$6.3^{+1.1}_{-1.0}$	$-3.0^{+0.3}_{-0.4}$	$-3.5^{+0.4}_{-0.3}$	$-1.5^{+0.8}_{-1.0}$	1.3
Aoki11	300, 400	2.5(7)	−2.8(3)	1.1	$2.1^{+3.8}_{-1.2}$	$-3.0^{+0.5}_{-1.9}$	$-3.2^{+1.2}_{-0.6}$	$0.7^{+0.7}_{-6.3}$	1.4
Alexandrou17	317	2.8(8)	−3.8(3)	0.6	$13.3^{+0.8}_{-0.4}$	$-12.9^{+0.5}_{-0.3}$	$15.0^{+0.3}_{-0.1}$	$-11.7^{+0.7}_{-0.4}$	0.7
Strategy (c)	≤ 320	-	-	-	$4.7^{+0.5}_{-0.2}$	$-2.9^{+0.09}_{-0.03}$	$-3.27^{+0.07}_{-0.03}$	$0.64^{(f)}$	2.1
Strategy (d)	236, 391	2.0(2)	−3.6(1)	1.1	-	-	-	-	-
Guo16 ($N_f = 2$)	226, 315	2.26(14)	−3.44(3)	1.3	-	-	-	-	-
Experimental	138	0.26(5)	−3.96(4)	-	0.26(5)	−3.96(4)	−3.01(2)	0.64(3)	-

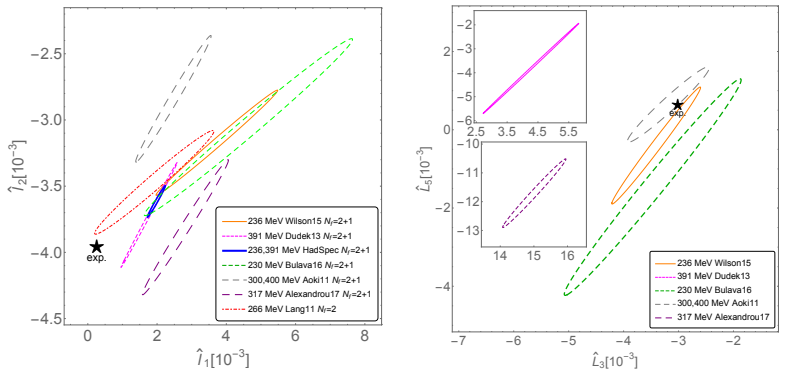

Figure 3. Left: Error ellipses (68% confidence) in the minimization (a) for the SU(3) analyses of the different lattice data sets from Refs. [20–22, 24, 28] (all $N_f = 2 + 1$). The thick blue line shows the ellipse for strategy (d). The red dash-dotted ellipse (Lang11) represents the uncertainties from the analysis of the $N_f = 2$ data of Ref. [33]; see Ref. [18]. The star stands for the result obtained in the fit to the experimental data (very small uncertainties, not shown). Right: Left: Error ellipses (68% confidence) for L_3 and L_5 in the minimization strategy (b) compared to the values obtained from the experimental fit (star).

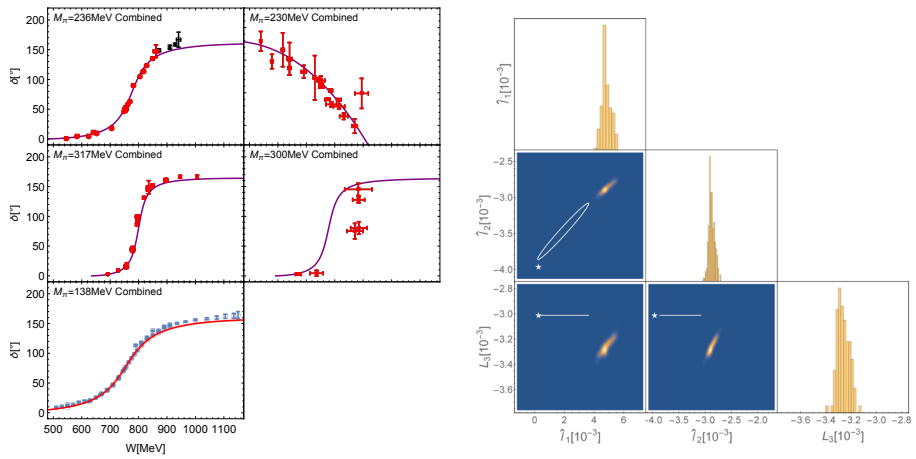

Figure 4. Left panel: Phase shifts obtained for the minimization strategy (c) described in the text. Lattice data included in the fit [21, 22, 24, 28] are highlighted in red. The extrapolation to the physical point in comparison to the experimental data (blue) [32] is shown in the bottom figure. Right: Density histogram from resampling obtained in minimization (c). Ellipses in white show the result obtained in Ref. [18] for the fit of the $N_f = 2$ data of Ref. [33] (Lang11) using the SU(2) UChPT model. There, L_3 and L_5 were held fixed to their experimental values such that the corresponding ellipses degenerate to lines in the figure. The stars indicate the LECs obtained from experimental phase shifts. The diagonal elements show histograms for the distributions of $\hat{l}_1$, $\hat{l}_2$ and L_3.

(b) are shown. All the ellipses are close to the values of L_3 and L_5 obtained from the experimental fit, except for the Dudek13 and Alexandrou17 cases shown in the inset. In the latter cases, a good chiral extrapolation can only be achieved at the cost of very different values of the LECs.

Fit (c) – Combined data $M_\pi < 320$ MeV. Data from all lattice simulations with M_π smaller or equal to 320 MeV are fitted simultaneously, while L_5 is kept fixed to the value from the fit to the experimental data. In this case the number of minima found in strategy (b) is significantly reduced and we are able to pin down the values of the other low-energy constants with much higher precision. The obtained low-energy constants are shown in Table 1. Phase shifts are depicted in Fig. 4 (left). The UChPT model describes the lattice data consistently, except for the Aoki11 data ($M_\pi = 300$ MeV). These data appear in tension to the others within the present model. The chiral extrapolation to the physical point postdicts the experimental phase shifts rather well (lower left figure). The corresponding values of (m_ρ, g) are shown in Fig. 2 (right) as red hexagon. The value of m_ρ is compatible with the physical one. To show the correlations between the parameters, density histograms obtained from resampling are displayed in Fig. 4 (right) for different pairs of low-energy constants. The ellipse show the results from the analysis of Ref. [18] of the $N_f = 2$ data from Lang *et al.* [33]. The star stands for the result from the experimental fit. The uncertainty region (light areas) obtained from fit (c) does not overlap with the result from the $N_f = 2$ analysis, which is also closer to the experiment.

Fit (d) – combined data Hadron Spectrum. The Hadron Spectrum Collaboration provides phase shifts for the ρ meson at two different pion masses of 236 and 391 MeV [20, 21]. We fit these data simultanously with L_3 and L_5 fixed as in minimization (a). The quality of the fit is indeed very good, with a $\chi^2_{\text{d.o.f}} = 1.1$, although the extrapolated ρ mass, ~ 750 MeV, turns out to be slightly lower than the experimental value, see Fig. 2 (left). The LECs obtained in this strategy are given in Table 1. They are remarkably close to the values obtained in $N_f = 2$ fits [17, 18]. Notice that $\hat{l}_1$ which is related to the ρ mass [17] has been reduced a factor 2-3 from the result obtained for these sets in minimization

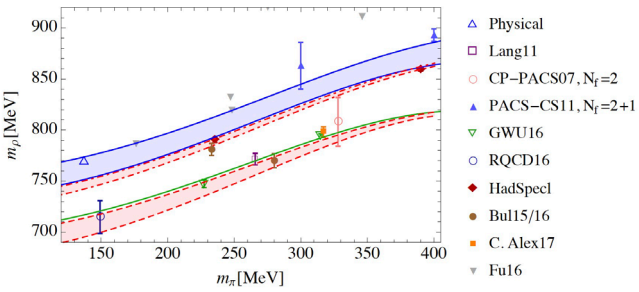

Figure 5. Red dot-dashed upper band: Pion mass dependence of the ρ mass from the combined fit of the $N_f = 2 + 1$ Hadron Spectrum data [20, 21] [minimization strategy (d)]. Lower red dashed band: Same but with $K\bar{K}$ channel removed. Green line: Analysis of $N_f = 2$ data of Ref. [17]. Blue solid band: Same but with $K\bar{K}$ channel added. $N_f = 2$ lattice results: Lang11, CP-PACS07, GWU16, RQCD16; $N_f = 2+1$: HadSpec (Dudek13, Wilson15), Bulava15, Bulava16, Alexandrou17, Fu16 (no error bars provided).

strategies (b) (chiral extrapolation compatible with experiment) and (c) (where Alexandrou17 and Aoki11 data sets are included), being now closer to the result from $N_f = 2$ analysis and experiment. With the values of the LECs obtained in this strategy, the pion mass dependence of the ρ is plotted in Fig. 5, in comparison with that from the analysis of Ref. [17], and with the lattice data. The $N_f = 2+1$ Alexandrou17 ρ mass (orange filled square at $M_\pi = 317$ MeV) is below the prediction of fit (d) and, in fact, very close to the $N_f = 2$ GWU result at similar mass. The $N_f = 2 + 1$ ρ masses of the Fu16 data [27] are larger than the predictions of fit (d) which could be related to a rather different value of the kaon mass or other problems (see discussion in Appendix).

To simulate the absence of the strange quark one can remove the $K\bar{K}$ channel from the result of fit (d). The red dashed band is obtained predicting consistently lighter ρ masses that are indeed compatible with most of the $N_f = 2$ data shown in the figure (Lang11 [33], CP-PACS07 [34], GWU16 [17], RQCD16 [19]).

In Ref. [17], the $K\bar{K}$ channel was included after fitting the $N_f = 2$ GWU16 data to simulate the missing strange quark of the lattice results. The outcome, including systematic model uncertainties, is shown with the blue solid band in Fig. 5. A substantial shift of the ρ mass was observed, this time to larger values. The outcome is in agreement with the physical ρ mass and, marginally, with fit (d).

4 Conclusions

The present analysis shows that UChPT can be used to parametrize the light-quark (or pion mass) dependence of the phase-shifts in the rho-channel well. In most of the $N_f = 2 + 1$ simulations, the extrapolation to the physical point of the mass is close to the experimental value. Still, the analysis reveals inconsistencies between some of the $N_f = 2 + 1$ data. Particularly, the Alexandrou17 (where the extrapolated ρ mass is significantly lower) and Fu16 (unknown value of the kaon mass) data sets, produce inconsistent results with other sets within our model. We also found that the LECs from a combined fit of the Hadron Spectrum Collaboration data for two different pion masses are in agreement with the ones of $N_f = 2$ UChPT analyses, and that, when the $K\bar{K}$ channel is removed, the value of the mass of the ρ shifted downwards, in good agreement with most of the $N_f = 2$ simulations and with the results found in Refs. [17, 18]. This further shows that the disagreement between the extrapolation of the $N_f = 2$ lattice results and the experiment is not an artifact of the extrapolation. As a further research direction, a combined fit to lattice data in other partial waves and, e.g., other

channels, πK, $K\bar{K}$,... could put tighter constraints on the LECs and show whether our UChPT model accurately captures the low-energy dynamics in meson-meson scattering across all channels.

References

[1] T. N. Truong, Phys. Rev. Lett. **61**, 2526 (1988)
[2] A. Gomez Nicola, J. R. Peláez and G. Ríos, Phys. Rev. D **77**, 056006 (2008)
[3] J. R. Peláez and G. Ríos, Phys. Rev. Lett. **97**, 242002 (2006)
[4] J. R. Peláez and G. Ríos, Phys. Rev. D **82**, 114002 (2010)
[5] A. Gomez Nicola and J. R. Peláez, Phys. Rev. D **65**, 054009 (2002).
[6] J. Nebreda and J. R. Peláez., Phys. Rev. D **81**, 054035 (2010)
[7] X. K. Guo, Z. H. Guo, J. A. Oller and J. J. Sanz-Cillero, JHEP **1506**, 175 (2015)
[8] Z. H. Guo, J. A. Oller and J. Ruiz de Elvira, Phys. Lett. B **712**, 407 (2012)
[9] J. Gasser and H. Leutwyler, Annals Phys. **158**, 142 (1984)
[10] J. Gasser and H. Leutwyler, Nucl. Phys. B **250**, 465 (1985)
[11] J. A. Oller, E. Oset and J. R. Peláez, Phys. Rev. D **59**, 074001 (1999) Erratum: [Phys. Rev. D **60**, 099906 (1999)] Erratum: [Phys. Rev. D **75**, 099903 (2007)].
[12] V. Bernard, M. Lage, U.-G. Meißner and A. Rusetsky, JHEP **1101**, 019 (2011)
[13] M. Döring, U.-G. Meißner, E. Oset and A. Rusetsky, Eur. Phys. J. A **47**, 139 (2011)
[14] M. Döring, J. Haidenbauer, U.-G. Meißner and A. Rusetsky, Eur. Phys. J. A **47** (2011) 163
[15] M. Döring, C. Hanhart, F. Huang, S. Krewald and U.-G. Meißner, Phys. Lett. B **681** (2009) 26
[16] M. Döring, U.-G. Meißner, E. Oset and A. Rusetsky, Eur. Phys. J. A **48**, 114 (2012)
[17] D. Guo, A. Alexandru, R. Molina and M. Döring, Phys. Rev. D **94**, no. 3, 034501 (2016)
[18] B. Hu, R. Molina, M. Döring and A. Alexandru, Phys. Rev. Lett. **117**, no. 12, 122001 (2016)
[19] G. S. Bali *et al.* [RQCD Collaboration], Phys. Rev. D **93**, 054509 (2016)
[20] J. J. Dudek *et al.* [Hadron Spectrum Collaboration], Phys. Rev. D **87**, no. 3, 034505 (2013)
[21] D. J. Wilson, R. A. Briceño, J. J. Dudek, R. G. Edwards and C. E. Thomas, Phys. Rev. D **92**, no. 9, 094502 (2015)
[22] J. Bulava, B. Fahy, B. Hörz, K. J. Juge, C. Morningstar and C. H. Wong, Nucl. Phys. B **910**, 842 (2016)
[23] J. Bulava, B. Hörz, B. Fahy, K. J. Juge, C. Morningstar and C. H. Wong, PoS LATTICE **2015**, 069 (2016)
[24] S. Aoki *et al.* [CS Collaboration], Phys. Rev. D **84**, 094505 (2011)
[25] B. Fahy, J. Bulava, B. Hörz, K. J. Juge, C. Morningstar and C. H. Wong, PoS LATTICE **2014**, 077 (2015)
[26] X. Feng, S. Aoki, S. Hashimoto and T. Kaneko, Phys. Rev. D **91**, no. 5, 054504 (2015)
[27] Z. Fu and L. Wang, Phys. Rev. D **94**, no. 3, 034505 (2016)
[28] C. Alexandrou *et al.*, arXiv:1704.05439 [hep-lat].
[29] T. Metivet [Budapest-Marseille-Wuppertal Collaboration], PoS LATTICE **2014**, 079 (2015)
[30] M. Döring, U.-G. Meißner and W. Wang, JHEP **1310**, 011 (2013)
[31] B. Hu, R. Molina, M. Döring, M. Mai and A. Alexandru, Phys. Rev. D **96**, no. 3, 034520 (2017)
[32] S. D. Protopopescu *et al.*, Phys. Rev. D **7**, 1279 (1973)
[33] C. B. Lang, D. Mohler, S. Prelovsek and M. Vidmar, Phys. Rev. D **84**, 054503 (2011) Erratum: [Phys. Rev. D **89**, 059903 (2014)]
[34] S. Aoki *et al.* [CP-PACS Collaboration], Phys. Rev. D **76**, 094506 (2007)